

Compact Modeling of the Noise of a Bipolar Transistor Under DC and AC Current Crowding Conditions

Jeroen C. J. Paasschens

Abstract—The effect of current crowding on dc, on ac, and in particular on the noise characteristic of bipolar transistors, is studied. An equivalent circuit able to model these effects is presented. General formulations to calculate current crowding in arbitrary geometries are derived. Both rectangular and circular geometries are discussed in detail.

Index Terms—Analog simulation, bipolar transistors, current crowding, equivalent circuits, noise, spice.

I. INTRODUCTION

RECENTLY, modeling the noise of bipolar transistors has received a lot of attention. This modeling is necessary for accurate prediction of noise behavior in radio frequency (RF) circuits. In a number of papers, the minimum noise figure and other quantities are being calculated from currents and resistances [1]–[4], or in terms of Y -parameters [5], [6]. All of these models predict the noise in terms of the measured (or modeled) currents and small-signal parameters, such that there is no need for difficult noise measurements. Compact transistor models [7], [8] like Mextram [9] and Hicum [10] predict dc, ac and noise behavior based on a number of extracted parameters. Preferably, also these parameters can be extracted without noise measurements.

Crucial for the development of these models is a good understanding of: 1) the microscopic noise sources of a bipolar transistor and 2) the transfer of these sources to the transistor terminals. Unfortunately, not all details are being understood, as is argued in [11]. Furthermore, not a lot of attention has been paid to the effect that current crowding has on the noise behavior. Some of the older literature discusses the subject [12]–[15] and even some experimental results are available [16]. In the light of recent noise modeling developments, it is necessary to reconsider the effect of current crowding on noise again. It should be noted that for modern transistors, dc current crowding is often not relevant for the smallest emitter widths, although for larger emitter widths it can be significant.

Our goal is to give a compact transistor model consisting of an equivalent transistor circuit suited for dc, ac, and noise simulations, and expressions for each of its elements. The model

should give the same behavior as the transistor which has a distributed base resistance. Furthermore, we would like the model to be simple.

We will show that the equivalent circuit that is being used in most compact models is actually sufficient. For dc and ac operation this is not surprising, since it is already being used extensively. We do present for the first time an emitter-geometry independent analysis, which can then be used to consider specific geometries. The fact that the simple standard equivalent circuit is sufficient to also describe the effect of current crowding on the noise is new. Previous publications [12]–[15] use more complicated equivalent circuits, having extra internal nodes.

In fact, we show that modeling the current crowding does not affect the intrinsic model. All of the current-crowding effects can be modeled by elements between the intrinsic and extrinsic base nodes. Furthermore, both for the dc and noise behavior, these elements do not depend on the elements of the intrinsic model. This also means that we get less correlated noise sources, compared to earlier analysis, which simplifies implementation in circuit simulators. This not only makes the modeling of current crowding itself simpler, it also gives much more freedom in making the intrinsic transistor model, because it becomes independent of the current-crowding model.

After the general analysis, we show explicit results for the circular emitter (which results in analytical expressions) and the rectangular emitter (for which we find interpolation formulas for implementation into a compact model).

Although we take a simple intrinsic transistor model in our analysis, we will argue that many of the other effects, like Early-effect, base-charge modulation, base-collector charge, and avalanche current do not change the model needed to describe current crowding effects.

II. CURRENT CROWDING

Current crowding is a result of the difference in base resistance that the various current paths of the transistor see. In Fig. 1, we show a schematic cross-section of the transistor. The corresponding schematic circuit is shown in Fig. 2. The resistance discussed here is the resistance of the pinched base; that part of the base that is under the emitter.

In dc operation, the difference in voltage drop over the pinched-base resistance leads to a larger forward bias close to the emitter perimeter than in the middle of the transistor, leading to a larger collector current density. When the collector-base bias is very large the base current can become negative due to

Manuscript received January 12, 2004; revised May 4, 2004. The review of this paper was arranged by Editor M. J. Deen.

The author is with Philips Research Laboratories, 5656 AA Eindhoven, The Netherlands (e-mail: jeroen.paasschens@philips.com).

Digital Object Identifier 10.1109/TED.2004.833580

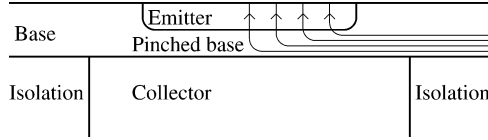


Fig. 1. Schematic cross section of the distributed transistor. Current crowding effects take place in the pinched base region. Schematic base current flow lines in half of the transistor are depicted.

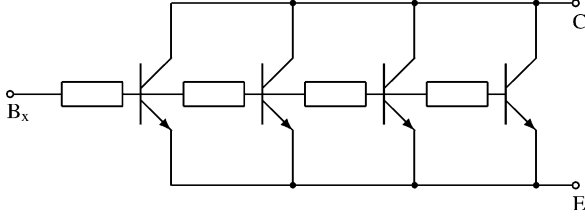


Fig. 2. Schematic circuit representation of the distributed transistor, where parts of the transistor at different locations see different total resistances to the base node B_x . The situation depicted here shows the distribution along only one dimension, using only four discrete resistors. In our analysis, we consider a continuous distribution of resistance and the more general case of crowding in two dimensions.

avalanche, and pinch-in occurs [17], [18]. In ac operation, the resistance has a similar effect.

Both dc and ac current crowding have an effect on the amount of resistance the base current sees while going from base to emitter. Both will therefore also have an effect on the amount of thermal noise of the base that is transferred to the terminals. (The amount of thermal noise generated is independent of current flow. Not all of that thermal noise is transferred to the terminals, however.)

III. INTRINSIC TRANSISTOR

Before we go to the full calculation of the distributed transistor, we first give the equations of the intrinsic transistor, i.e., without base resistance. Its equivalent circuit is shown in Fig. 3. The expressions of the intrinsic transistor will be the basis of the distributed approach of the next section, in which a lot of intrinsic transistors are connected via the base resistance, as shown in Fig. 2.

A. DC Behavior

For the dc currents, we write

$$I_C = I_s e^{V_{B_1E}/V_T}; \quad I_B = \frac{I_s}{\beta} e^{V_{B_1E}/V_T}. \quad (1)$$

Here, $V_T = k_B T/q$ is the thermal voltage, I_s is the saturation current and β is the current gain. Because the nonideal base current is often only relevant at low currents, we neglect it. A description of the noise in the nonideal base currents (relevant in for instance III-V HBT's) is difficult because those currents are no longer dominated by diffusion. They are therefore outside the scope of this paper. For a discussion about high-current effects, see Section IX.

B. AC Behavior

For the discussion about the ac behavior (and also the noise behavior discussed below), we show the small-signal version of

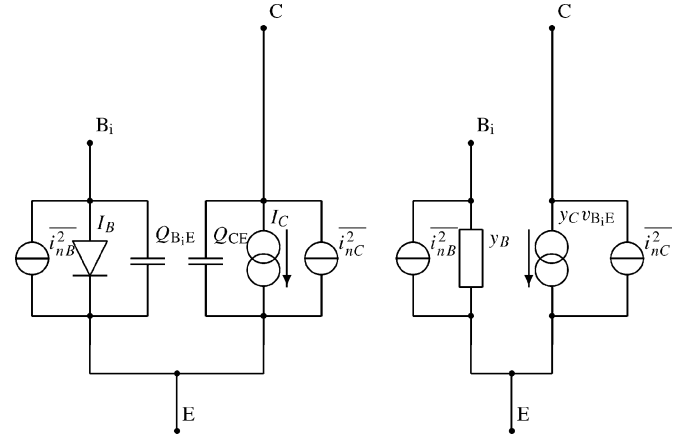


Fig. 3. Equivalent circuit for the intrinsic transistor. On the left the large-signal circuit, on the right the small-signal circuit. The base node of this intrinsic transistor is called B_1 , to distinguish it from the node B_x of the distributed transistor in Fig. 2. The charge Q_{CE} models base-charge partitioning. For a discussion of other relevant elements like the base-collector charge and avalanche current, see Section IX.

the equivalent circuit in Fig. 3. For the intrinsic transistor, we take

$$y_B = \frac{I_B}{V_T} + j\omega \cdot \frac{dQ_{B_1E}}{dV_{B_1E}} \simeq \gamma_B(\omega)g_B. \quad (2)$$

The limit for zero frequency of y_B is $g_B = I_B/V_T$. The last step, where we give the base-admittance y_B as a frequency-dependent factor $\gamma_B(\omega)$ times the voltage dependent term g_B , is a good approximation, as was argued in [14]. Note that this general way of presenting also allows a simple extension to higher order frequency effects, if needed.

In the practice of compact modeling, only first-order frequency effects are taken into account because of the implementation in terms of charges. For those situations, we can write $\gamma_B = (1 + j\omega\tau)$. The effective transit time τ can be found from (2). This approximation should be enough for frequencies such that $\omega\tau \ll 1$, which means for frequencies well below the maximal cutoff frequency.

Also in the small-signal collector current a charge contribution can be present. Although we will neglect base-collector (depletion) capacitance contributions for the moment (see Section IX), there can be a contribution due to charge partitioning (related to excess phase shift). This contribution also depends exponentially on the voltage. The small-signal collector admittance is therefore similar to that of the base

$$y_C = \gamma_C(\omega)g_m \quad (3)$$

where the transconductance $g_m = I_C/V_T = \beta g_B$ is the zero-frequency limit of y_C .

C. Noise Behavior

The thermal noise of the intrinsic transistor manifests itself as shot-noise, where the noise density is proportional to $2qI$. Transit time effects in the base affect the transfer from the local noise sources to the terminals [19]–[22], see also [23], [24]. As

as a result, the base and collector current shot-noise terms become frequency dependent and correlated

$$\overline{i_{nC}i_{nC}^*} = \gamma_{n,CC}(\omega) \cdot 2qI_C\Delta f \quad (4a)$$

$$\overline{i_{nB}i_{nB}^*} = \gamma_{n,BB}(\omega) \cdot 2qI_B\Delta f \quad (4b)$$

$$\overline{i_{nB}i_{nC}^*} = \gamma_{n,BC}(\omega) \cdot 2qI_C\Delta f. \quad (4c)$$

The factors $\gamma_{n,BB}$ and $\gamma_{n,CC}$ are real, whereas $\gamma_{n,BC}$ is complex. We assume the various pre-factors γ bias-independent, as far as the analysis of current-crowding is concerned, just as many other terms, see Section IX. In the limit of zero frequency $\gamma_{n,BB} = \gamma_{n,CC} = 1$ and $\gamma_{n,BC} = 0$, which gives the familiar relations implemented in most compact models.

IV. DISTRIBUTED APPROACH

In this section, we consider the distributed transistor shown in Fig. 2. The results of this section will be used to define the elements in the much simpler equivalent circuit of Section V.

The distributed transistor of Fig. 2 has a total base current I_{TB} and a total collector current I_{TC} , as well as a total base current noise source i_{TB} and i_{TC} , shown schematically in Fig. 4. Furthermore, the transistor has small-signal admittances $y_{11} = y_{TB}$ and $y_{21} = y_{TC}$ (we disregard output and feedback admittances y_{22} and y_{12} for now). In this section, we will derive expressions for these quantities.

A. DC Current Crowding

DC current crowding has already been discussed in many publications [25]–[32]. Therefore, we only need to state our assumptions and notation, but also give the equations we will need further on. In extension to previous publications, we will consider a general shape of the emitter area.

We consider the two-dimensional base current flow in the pinched base, which has a sheet resistance ρ . We assume this flow to be lateral under the emitter region, having an area A_{em} . The lateral current density in the base is denoted by \mathbf{J} (dimension A/m). At each position in the base the transversal current density J_{BE} (dimension A/m²) that goes from the base to the emitter is given by a simple exponential relation, that depends on the difference $V(\mathbf{r}) = V_B(\mathbf{r}) - V_E$ between the local base voltage $V_B(\mathbf{r})$ and the constant emitter voltage V_E

$$J_{BE}(V) = \frac{I_s}{A_{em}\beta} e^{V/V_T}. \quad (5)$$

Note that the current density J_{BE} flows perpendicular to \mathbf{J} .

The equations that describe dc current crowding are then Ohm's law and a continuity equation, respectively

$$\nabla V = -\rho\mathbf{J} \quad (6a)$$

$$\nabla \cdot \mathbf{J} = -J_{BE}(V). \quad (6b)$$

The total base current can be expressed as

$$I_B = \int_{A_{em}} J_{BE}[V(\mathbf{r})]d\mathbf{r}. \quad (7)$$

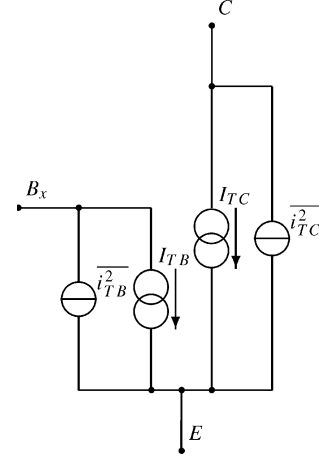


Fig. 4. Circuit which gives the total currents and total current noise sources for the part of the transistor including the intrinsic transistor and the resistance of the pinched base. The charge contributions are not shown.

The integral here and all integrals below are over all of the emitter area. Because the current gain β is taken constant over the base, the local and therefore also the total collector current is proportional to the base current

$$I_C = \beta I_B. \quad (8)$$

The differential equation for the voltage can be found from (6) by eliminating the current density

$$\nabla^2 V = \rho J_{BE}[V(\mathbf{r})]. \quad (9)$$

We need to solve this equation under the condition that $V = V_{BxE}$ everywhere on the boundary of the pinched base. (Another condition is that there are no singularities in the solution, which we need in for instance circular geometries.)

The solution of (9) will form the basis of the small-signal and noise analysis below. In Sections VII and VIII, we present explicit results.

B. AC Current Crowding

The small-signal equations can be found from (6) by adding a small-signal component to both the voltage ($V \rightarrow V + v$) and the current densities ($\mathbf{J} \rightarrow \mathbf{J} + \mathbf{j}$ and $J_{BE} \rightarrow J_{BE} + j_{BE}$). The equations for the small-signal terms then become

$$\nabla v = -\rho\mathbf{j}, \quad \nabla \cdot \mathbf{j} = -j_{BE}(\mathbf{r}). \quad (10)$$

The small-signal current j_{BE} is found from the small-signal behavior of the intrinsic transistor

$$j_{BE}(\mathbf{r}) = \frac{\gamma_B(\omega)J_{BE}(\mathbf{r})v(\mathbf{r})}{V_T}. \quad (11)$$

The differential equation for v can then be found from (10)

$$\nabla^2 v = \frac{\rho}{V_T}\gamma_B(\omega)J_{BE}(\mathbf{r})v(\mathbf{r}) \quad (12)$$

with $v(\mathbf{r}) = v_{BxE}$ for any point on the boundary.

The small-signal variation in the voltage also leads to a change in the base current ($I_B \rightarrow I_B + i_B$). The expression for i_B is, using (11)

$$i_B = \int_{A_{em}} j_{BE}(\mathbf{r}) d\mathbf{r} = \left(\frac{\gamma_B}{V_T} \right) \int_{A_{em}} J_{BE}(\mathbf{r}) v(\mathbf{r}) d\mathbf{r}. \quad (13)$$

For the noise analysis, we also need the small-signal collector current j_C , for which it holds that

$$\nabla \cdot \mathbf{j}_C = -\frac{\beta}{V_T} \gamma_C(\omega) J_{BE}(\mathbf{r}) v(\mathbf{r}). \quad (14)$$

The total small-signal collector current i_C is then

$$i_C = \frac{\beta}{V_T} \gamma_C(\omega) \int_{A_{em}} J_{BE}(\mathbf{r}) v(\mathbf{r}) d\mathbf{r} = \frac{\beta \gamma_C(\omega)}{\gamma_B(\omega)} i_B. \quad (15)$$

As one can see, the ratio between the total small-signal collector and base currents is the same as in the intrinsic model. The admittances are now $y_{TB} = i_B/v_{B_xE}$ and $y_{TC} = i_C/v_{B_xE}$.

C. Noise Behavior

To discuss the distributed noise effects, we start with the small-signal equations above. We then add the Langevin noise sources e_{nR} , j_{nB} , and j_{nC} , representing the noise of the base resistance and the base and collector shot noise currents, respectively. The equations we get are

$$\nabla v_n = -\rho \mathbf{j} + e_{nR}(\mathbf{r}) \quad (16a)$$

$$\nabla \cdot \mathbf{j} = -\frac{1}{V_T} \gamma_B(\omega) J_{BE}(\mathbf{r}) v_n(\mathbf{r}) - j_{nB}(\mathbf{r}) \quad (16b)$$

$$\nabla \cdot \mathbf{j}_C = -\frac{\beta}{V_T} \gamma_C(\omega) J_{BE}(\mathbf{r}) v_n(\mathbf{r}) - j_{nC}(\mathbf{r}) \quad (16c)$$

where $v_n(\mathbf{r})$ is the noise voltage that is to be determined. (Here we use v_n instead of v for distinction with the ac analysis.) The boundary condition we use is $v_{B_xE} = 0$. This means that $v_n(\mathbf{r}) = 0$ on all points on the boundary.

Before we solve (16) we need to give the statistical properties of the Langevin noise sources. We start with the shot-noise terms j_{nB} and j_{nC} . Locally, these should give the same results as that of the intrinsic model, given in (4). This means that $\overline{j_{nB} j_{nB}^*}$ should be proportional to the local current density from base to emitter $J_{BE}(V)$, with of course a pre-factor $2q\Delta f$. Furthermore, the noise should be local, which means that the noise at one position \mathbf{r} is not correlated to another position \mathbf{r}' . This results in

$$\overline{j_{nB} j_{nB}^*} = \gamma_{n, BB}(\omega) \cdot 2q J_{BE}(\mathbf{r}) \delta(\mathbf{r} - \mathbf{r}') \Delta f \quad (17a)$$

$$\overline{j_{nC} j_{nC}^*} = \gamma_{n, CC}(\omega) \cdot 2q \beta J_{BE}(\mathbf{r}) \delta(\mathbf{r} - \mathbf{r}') \Delta f \quad (17b)$$

$$\overline{j_{nB} j_{nC}^*} = \gamma_{n, BC}(\omega) \cdot 2q \beta J_{BE}(\mathbf{r}) \delta(\mathbf{r} - \mathbf{r}') \Delta f. \quad (17c)$$

Here, $\delta(\mathbf{r} - \mathbf{r}')$ is the Dirac delta function.

The other noise source e_{nR} is simply a voltage noise source describing thermal noise. It is therefore proportional to $4k_B T \Delta f$ times the local resistance

$$\overline{(e_{nR})_p(\mathbf{r}) (e_{nR})_q^*(\mathbf{r}')} = 4k_B T \rho \delta(\mathbf{r} - \mathbf{r}') \delta_{pq} \Delta f \quad (18)$$

where δ_{pq} is the Kronecker delta ($\delta_{pq} = 1$ only when $p = q$ and zero otherwise). The thermal noise term e_{nR} is uncorrelated to j_{nB} and j_{nC} . Correlation in the extrinsic currents results from interaction of the noise sources and the rest of the equivalent circuit.

Now that the noise sources are given, we can return to the solution of the set of differential equations (16). The formal solution of the voltage is given in Appendix A. We do not need an actual expression for v_n . The total current noise sources i_{TB} and i_{TC} can be expressed in terms of the auxiliary function $y_s(\mathbf{r})$. This y_s can be found in terms of the solution of (12) as

$$y_s(\mathbf{r}) = \frac{\left[1 - \frac{v(\mathbf{r})}{v_{B_xE}} \right]}{\gamma_B(\omega)} \quad (19)$$

(see Appendix A). This means that to be able to find usable expressions for the noise, we first need the ac (and dc) solutions for the same transistor geometry.

The result for the total current noise sources, as derived in Appendix A, is

$$i_{TB} = \frac{\gamma_B(\omega)}{\rho} \int e_{nR}(\mathbf{r}) \cdot \nabla y_s(\mathbf{r}) d\mathbf{r} + \int j_{nB}(\mathbf{r}) [1 - \gamma_B(\omega) y_s(\mathbf{r})] d\mathbf{r} \quad (20a)$$

$$i_{TC} = \frac{\beta \gamma_C(\omega)}{\rho} \int e_{nR}(\mathbf{r}) \cdot \nabla y_s(\mathbf{r}) d\mathbf{r} - \beta \gamma_C(\omega) \int j_{nB}(\mathbf{r}) y_s(\mathbf{r}) d\mathbf{r} + \int j_{nC}(\mathbf{r}) d\mathbf{r}. \quad (20b)$$

These solutions will be used in the following sections to find the noise sources of the simpler equivalent circuit.

V. EQUIVALENT CIRCUIT

The behavior of the distributed transistor has been given in the previous section. We now have to give an equivalent circuit with expressions for all its elements, that gives the same behavior as the distributed transistor. In this section, we will discuss the equivalent circuit. In the next section we will then derive the expressions for all elements.

In Fig. 5, we show the equivalent circuit we propose. This equivalent circuit is already used in advanced compact models [7], [8], like Mextram [9] and Hicum [10]. For a complete model, more elements are needed—see Section IX.

The added value of our work is not so much in the equivalent circuit of Fig. 5. As mentioned, the equivalent circuit is already being used. Rather, we will show that all intrinsic elements (i.e., the ones between nodes B_i and E or between nodes C and E) do *not* contain current crowding effects. In other words, these elements are the ones one would have in case there was no base resistance at all. They are discussed in Section III. All current crowding effects can be modeled by the elements between the extrinsic and intrinsic base nodes B_x and B_i . Especially for analytical noise modeling, this approach is new.

Many models for the base-resistance exist (see [29] for various definitions of base-resistance and [30] for a comparison of

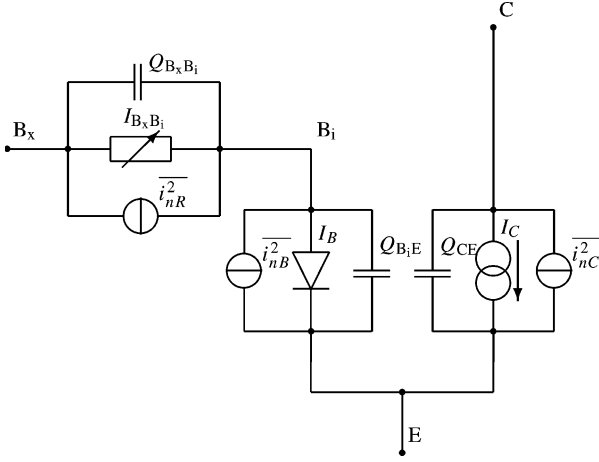


Fig. 5. Equivalent circuit we propose for the intrinsic transistor together with the resistance of the pinched base. In practice, the diode-like currents I_B and I_C are implemented as nonlinear voltage-controlled current sources. For a discussion of other relevant elements like the base-collector charge and avalanche current, see Section IX.

various models). We find that the most practical way to implement the variable resistance is to use a voltage controlled current source I_{B_x, B_i} . Implementing a current-controlled voltage source [31] will often lead to an extra degree of freedom in a simulator. We will show below that for the calculation of the noise one can use neither the dc nor the ac resistance.

The charge Q_{B_x, B_i} is also nonlinear, just as the charges $Q_{B_i, E}$, Q_{CE} . Whereas the current I_{B_x, B_i} only depends on the voltage V_{B_x, B_i} , the charge Q_{B_x, B_i} depends also on $V_{B_i, E}$ (via the derivatives of $Q_{B_i, E}$), as we will show below.

In literature, two equivalent circuits for modeling crowding effects in the noise have been presented. For the single-sided (or double-sided) contacted base, the equivalent circuit used in [12] and [13] has the disadvantage that the resistance of the pinched base is split into two parts, adding an extra node to the circuit. Another equivalent circuit was introduced for a circular geometry [14], but later used for rectangular geometries as well in [15] (in which it is also argued that expressions found in [12], [13] were inexact). This equivalent circuit is unnecessarily complex. In both equivalent circuits, many of the noise sources are correlated to other noise sources. The only correlation that needs to be taken into account in our approach is the correlation in the intrinsic transistor that would be there even without base resistance, see Section VI-C. Even though the current noise source i_{nR} is uncorrelated to the other noise sources, the equivalent circuit takes care of correlation that exists between the external noise sources i_{TB} and i_{TC} . It is important to realize that i_{nR} , which depends only on the voltage V_{B_x, B_i} and not on parts of the intrinsic transistor, contains contributions from both the thermal noise e_{nR} and shot-noise j_{nB} .

VI. LUMPED APPROACH

In this section, we will derive the expressions for all the elements in the lumped circuit given in Fig. 5 in such a way that the behavior of the lumped circuit is the same as that of the distributed transistor of Fig. 2 or Fig. 4.

A. DC Behavior

Let us first consider the dc behavior of our lumped approach. For the collector and base currents, we will use the same expressions as for the intrinsic model, i.e (1). The condition that the collector current I_C and base current I_B need to be the same as the total collector current I_{TC} and total base current I_{TB} from Fig. 4, then determines the value of the voltage difference $V_{B_i, E}$.

Next we need to find a relation between the base current $I_B = I_{B_x, B_i}$ and the voltage difference V_{B_x, B_i} . The solution of the differential equation (9) gives an expression for $J_{BE}(\mathbf{r})$. If we take the value of J_{BE} at any point $\mathbf{r}_{\text{bound}}$ of the boundary of the pinched base we have, from the definition (5) of J_{BE} and the boundary condition, that

$$J_{BE}(\mathbf{r}_{\text{bound}}) = \frac{I_s}{A_{em}\beta} e^{V_{B_x, B_i}/V_T}. \quad (21)$$

Since the solution of (9) gives a relation between the base current I_B and V_{B_x, B_i} , it is possible to express $J_{BE}(\mathbf{r}_{\text{bound}})$ in terms of I_B . Eliminating I_s from (1) and (21), we find a relation for the voltage difference V_{B_x, B_i}

$$e^{V_{B_x, B_i}/V_T} = \frac{J_{BE}(\mathbf{r}_{\text{bound}})A_{em}}{I_B} \quad (22)$$

where the right-hand-side can be expressed as function of $I_B = I_{B_x, B_i}$. Equation (22) therefore gives the relation between I_{B_x, B_i} and V_{B_x, B_i} that we need for the implementation of a compact model. Many results have already been presented that give this relation in specific cases [25]–[32].

Note that it is possible that the relation between I_{B_x, B_i} and V_{B_x, B_i} is only implicit. In that case one needs to find a suitable approximation for use in the compact model. For example, in the rectangular emitter no explicit relation is available, and an approximation is needed—see Section VIII.

1) *Low-Current Limit:* For compact modeling, it is useful to express the relation between I_{B_x, B_i} and V_{B_x, B_i} in terms of the effective low-current resistance of the pinched base R_{Bv} . This R_{Bv} is defined as the low-current limit of $V_{B_x, B_i}/I_{B_x, B_i}$, and can be expressed as a geometry-dependent factor times the sheet resistance ρ . How this can be done for general geometries is shown in Appendix B. For a circular geometry, one has [27] $R_{Bv} = \rho/8\pi \simeq \rho/25.1$ (see also Section VII). For rectangular geometries with the base contacted on all four sides, our exact analytical result (73) from Appendix B is too complicated to be used in practice. A good approximation (based on simulations) has been given in [33] for general emitter width H_{em} over length L_{em} ratios

$$R_{Bv} \simeq \rho \frac{H_{em}}{L_{em}} \left[\frac{1}{12} - \left(\frac{1}{12} - \frac{1}{28.45} \right) \frac{H_{em}}{L_{em}} \right] \quad (23)$$

(we replaced the value 28.6 used in [33] by the more accurate value 28.45 we found in Appendix B). This approximation is less than 5% larger than our exact result for all values of $0 \leq H_{em} \leq L_{em}$, and approaches the exact result both for very long emitters and for square emitters.

B. AC Behavior

Also for the ac behavior, the elements of the intrinsic part of the transistor in Fig. 5 are taken the same as those of the circuit in Fig. 3. The small-signal version of the equivalent circuit is given in Fig. 6. The expressions for the intrinsic transistor given in Section III-B also remain unchanged. This is allowed because the ratio of the small-signal collector and base currents is not influenced by current crowding, as shown in Section IV-B, (15).

We need to determine the admittance y_R of the branch between nodes B_x and B_i . It can be found from the admittance y_{TB} of the total circuit, derived in Section IV-B, using $1/y_{TB} = 1/y_R + 1/y_B$. This results in

$$y_R = \frac{y_B y_{TB}}{y_B - y_{TB}}. \quad (24)$$

In the limit for zero frequency, we can make use of $y_B = g_B = dI_B/dV_{B_iE}$ and $y_{TB} = g_{TB} = dI_B/dV_{B_xE}$ to find the zero-frequency limit of y_R as $y_R = g_R \equiv dI_{B_xB_i}/dV_{B_xB_i}$. Hence, an expression for g_R can be found once the dc current crowding has been analyzed. For low currents (and voltages), we obviously have $g_R = 1/R_{B_x}$.

Apart from the conductance of the B_x - B_i branch, we also need to find the charge $Q_{B_xB_i}$. We do this by taking only terms up to the first order in frequency, such that we can write

$$y_R = g_R + j\omega C_{B_xB_i}. \quad (25)$$

Once we have determined y_R , we can find $C_{B_xB_i}$, and, at least in principle, integrate this to find the charge $Q_{B_xB_i}$.

Often the combination of dc current crowding (inhomogeneous current flow) and ac current crowding is too difficult to handle analytically. One then considers ac current crowding without dc current crowding. This leads to a normal R - C transmission line model (but for the moment in an arbitrary geometry) where the capacitance is given by the base-emitter capacitance $C_{B_iE} = dQ_{B_iE}/dV_{B_iE}$. For such a transmission line model the equivalent circuit at low frequencies contains a capacitance $C_{B_xB_i}$ that can be given by a factor a times the capacitance C_{B_iE} . The factor a depends on geometry only. In the case of a rectangular base it is $1/5$ [34], which is being used in many cases. For a circular geometry it is $1/3$, as we show in Section VII. The charge in the B_x - B_i branch can then be given as

$$Q_{B_xB_i} = a V_{B_xB_i} \frac{dQ_{B_iE}}{dV_{B_iE}}. \quad (26)$$

C. Noise Behavior

Next we consider the noise behavior. From our distributed analysis, we found expressions for i_{TB} and i_{TC} . We want to map these two expressions on the equivalent circuit of Fig. 5. This circuit contains three noise sources, so there is some freedom in doing this. From inspection of (20b) for i_{TC} follows

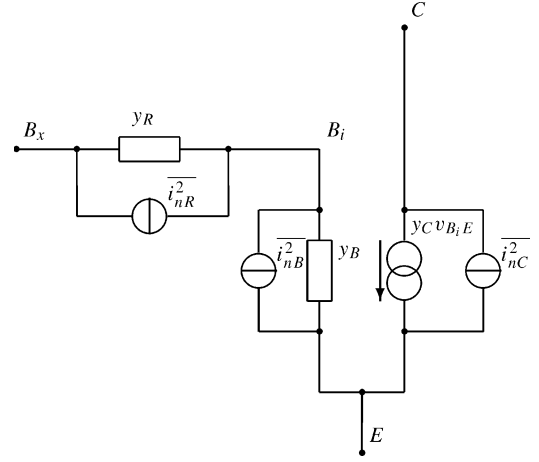


Fig. 6. Small-signal equivalent circuit belonging to the large-signal equivalent circuit of Fig. 5. Base-collector capacitance and excess phase shift are discussed in Section IX.

the natural choice to express the collector current noise source i_{nC} of the lumped circuit as

$$i_{nC} = \int_{A_{em}} j_{nC}(\mathbf{r}) d\mathbf{r}. \quad (27)$$

This equations tells us simply that the collector current noise source i_{nC} is just the unweighed sum of all local contributions. This choice for i_{nC} leads to a natural expressions for i_{nB} also and to zero correlation of both shot-noise sources with i_{nR} , as we will show next.

For the determination of the other two noise sources i_{nB} and i_{nR} , we consider the circuit in Fig. 6. From this circuit, we find the total noise sources in terms of the three elementary noise sources as

$$i_{TB} = i_{nB} \frac{y_R}{y_R + y_B} + i_{nR} \frac{y_B}{y_R + y_B} \quad (28a)$$

$$i_{TC} = i_{nC} + (i_{nR} - i_{nB}) \frac{y_C}{y_R + y_B}. \quad (28b)$$

The y -parameters of the small-signal circuit are known from the small-signal analysis. The two noise sources i_{nB} and i_{nR} of our equivalent circuit can then be found from

$$i_{nB} = i_{TB} - \frac{(i_{TC} - i_{nC}) y_B}{y_C} \quad (29a)$$

$$i_{nR} = i_{TB} + \frac{(i_{TC} - i_{nC}) y_R}{y_C}. \quad (29b)$$

For the base current noise source i_{nB} we find, using (20a) and (29)

$$i_{nB} = i_{TB} - (i_{TC} - i_{nC}) \frac{\gamma_B(\omega)}{\beta \gamma_C(\omega)} = \int_{A_{em}} j_{nB}(\mathbf{r}) d\mathbf{r}. \quad (30)$$

So also for the base current noise source, we find that it is just the unweighed sum of all local contributions.

The noise of the resistive part can also be found from (29), using the expressions (20) for i_{TB} and i_{TC}

$$i_{nR} = \frac{y_R + y_B}{\rho g_B} \int e_{nR}(\mathbf{r}) \cdot \nabla y_s(\mathbf{r}) d\mathbf{r} + \int j_{nB}(\mathbf{r}) \left[1 - \frac{y_R + y_B}{g_B} y_s(\mathbf{r}) \right] d\mathbf{r}. \quad (31)$$

Now that the three current noise sources are given, we can consider their statistical properties. Using the expressions for i_{nC} and the properties of the noise sources given in (17), we find

$$\begin{aligned} \overline{i_{nC} i_{nC}^*} &= \int \int \overline{j_{nC}(\mathbf{r}) j_{nC}^*(\mathbf{r}')} d\mathbf{r} d\mathbf{r}' \\ &= \gamma_{n,CC}(\omega) 2q\beta \int J_{BE}(\mathbf{r}) d\mathbf{r} \\ &= \gamma_{n,CC}(\omega) \cdot 2qI_C \Delta f. \end{aligned} \quad (32)$$

In the same way, we find $\overline{i_{nB} i_{nB}^*}$ and $\overline{i_{nB} i_{nC}^*}$. The resulting equations are the same as that of the intrinsic transistor we started with, given in (4). In Appendix C, we show that

$$\overline{i_{nR} i_{nB}^*} = \overline{i_{nR} i_{nC}^*} = 0. \quad (33)$$

In other words, in the lumped model the base and collector current shot noise sources, and the noise source parallel to the resistor are uncorrelated. The only average for which a simple expression cannot be given is $\overline{i_{nR} i_{nR}^*}$. We give a full expression in Appendix C. The relevant expression for compact modeling is discussed below.

As mentioned before in Section III-B, for compact modeling only terms up to the first order in frequency are relevant in practice. In general, all even-order terms of frequency dependent quantities are real; all uneven order terms are purely imaginary. This means that all real numbers do not have a first-order contribution in ω and are therefore independent of ω up to the first order. Up to the first order in frequency, we thus find $\gamma_{n,CC} = \gamma_{n,BB} = 1$. The noise equations in (4) then lead the well-known relations $\overline{i_{nB} i_{nB}^*} = 2qI_B \Delta f$ and $\overline{i_{nC} i_{nC}^*} = 2qI_C \Delta f$. When we consider the correlation between base and collector current noise sources, we can use that $\gamma_{n,BC}(\omega=0) = 0$. So for low frequencies $\gamma_{n,BC} \simeq j\omega\tau_n$, with τ_n a noise delay time [21], [22].

For the noise in the resistor-branch, we find from (77), up to the first order in frequency

$$\begin{aligned} \overline{i_{nR} i_{nR}^*} &= 2k_B T \left[(2g_R + g_B) - \frac{(g_R + g_B)^2}{V_T g_B^2} \int J_{BE}(\mathbf{r}) g_s(\mathbf{r})^2 d\mathbf{r} \right] \Delta f. \end{aligned} \quad (34)$$

Here, g_s is the zero-frequency limit of y_s , defined in (19), just as $g_B = y_B(\omega=0)$ and $g_R = y_R(\omega=0)$. Since the differential equation for g_s is simpler than that for y_s , it is easier to find solutions in particular geometries and from that calculate $\overline{i_{nR} i_{nR}^*}$. Whether we can find an expression for $\overline{i_{nR} i_{nR}^*}$ in practice depends very much on whether we can find a solution for $J_{BE}(\mathbf{r})$ and $g_s(\mathbf{r})$ in the first place, and if we can, whether $\int J_{BE} g_s^2 d\mathbf{r}$ can be integrated analytically. Only in the case of a circular emitter we were able to find a simple expression, which we give

in Section VII. For the rectangular geometry, we present an approximation in Section VIII.

VII. CIRCULAR GEOMETRY

In the previous sections, we have given formulations for describing the current crowding behavior in general geometries. Now we consider specific geometries, the results of which can be used in compact models. We start with the circular geometry, because this allows us to give analytical results [27]. Furthermore, a circular geometry can be relevant for small emitter sizes [31]. Most of our results are equivalent to those of [14], although our final results are simpler, mainly because our equivalent circuit is different (and also simpler) as discussed above.

A. Dc Current Crowding

In a circular geometry, we take the emitter to be located in the region $r \leq R_{em}$. The effective low-current resistance is $R_{Bv} = \rho/8\pi \simeq \rho/25.1$, comparable to that of a square emitter contacted on all sides, $R_{Bv} \simeq \rho/28.45$ —see Appendix B. The expressions we give below will be expressed in terms of

$$r_0^2 = R_{em}^2 \left(1 + \frac{V_T}{I_B R_{Bv}} \right). \quad (35)$$

Note that $r_0 > R_{em} \geq r$. The solution of dc current crowding is

$$J_{BE}[V(r)] = \frac{8V_T r_0^2}{\rho(r_0^2 - r^2)^2} \quad (36)$$

which can be verified by substitution in (9), using (5). Substituting the solution (36) in (22), we find the relation between current and voltage of the B_x - B_i branch

$$I_{B_x B_i} = \frac{V_T}{R_{Bv}} \left(e^{V_{B_x B_i}/V_T} - 1 \right) \quad (37)$$

expressed as a voltage-controlled current source.

B. AC Current Crowding

For the small-signal results, we can directly find $g_B = I_B/V_T$ and $g_R = g_B + 1/R_{Bv}$ from the dc solution given above. Next we consider the frequency dependence. We will take into account only terms up to the first order in frequency (see Section III-B) and write $\gamma_B(\omega) = 1 + j\omega\tau$. Blasquez [14] has given a solution for $v(r)$ from (12) in terms of a hyper-geometric series. For zero frequency the solution is $v(r) = v_0(r)$, with

$$v_0(r) = v_{BxE} \frac{(r_0^2 + r^2)(r_0^2 - R_{em}^2)}{(r_0^2 - r^2)(r_0^2 + R_{em}^2)}. \quad (38)$$

The solution of Blasquez [14] contains all orders in frequency. In our opinion, this is not useful if the starting point itself, i.e., γ_B , contains only the first order in frequency. Unfortunately, we were not able to take the low-frequency limit of the full expression directly. Instead, we solved the differential equation to the first order in frequency. The result is

$$v(r) = v_0(r) \left[1 - \frac{2}{3} j\omega\tau t(r) \right] \quad (39a)$$

$$t(r) = [1 - v_0(r)] \frac{r_0^2 - r^2}{r_0^2 + r^2} + \ln \left(\frac{r_0^2 - r^2}{r_0^2 - R_{em}^2} \right). \quad (39b)$$

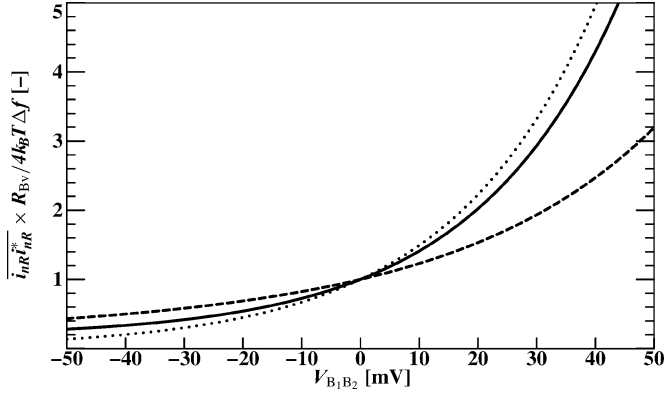


Fig. 7. Noise in the resistance branch $\overline{i_{nR}^*}$ in a circular geometry, normalized to the zero-bias value $4k_B T \Delta f / R_{Bv}$ for the exact solution (41) (solid) and the two incorrect results (42) (dashed) and (43) (dotted).

This result can be verified by substitution, and has, to our knowledge, not been presented before. Now that we have a solution of v , we can calculate y_R , using the results from Section IV-B. To the first order in frequency, we get

$$y_R = R_{Bv}^{-1} + g_B \left(1 + \frac{1}{3} j\omega\tau \right). \quad (40)$$

This factor 1/3 is different from the factor 1/5 found in rectangular geometries. Although for low currents this factor can be found from [14], we show here that it is valid for all current levels.

C. Noise Behavior

For the noise behavior the only quantity for which the calculation is nontrivial is $\overline{i_{nR}^*}$, which we can find from (34). For this we need $g_s(r) = 1 - v_0(r)/v_{B_x E}$, with v_0 given in (38). The result is

$$\begin{aligned} \overline{i_{nR}^*} &= \frac{4k_B T}{R_{Bv}} \Delta f \frac{5e^{V_{B_x B_i}/V_T} + 1}{6} \\ &= \frac{4k_B T}{R_{Bv}} \Delta f + \frac{10}{3} qI_B \Delta f. \end{aligned} \quad (41)$$

From this expression, one might think that the first term is due to the noise in the resistance, while the second term is due to the base shot noise. The contribution of the base shot noise to $\overline{i_{nR}^*}$ is, however, only $(2/3)qI_B \Delta f$, which can also be found from the results in [15].

We can compare the result (41) with the standard result $\overline{i_{nR}^*} = 4k_B T \Delta f / R$, with R the resistance. For this resistance one can take either the dc resistance $V_{B_x B_i} / I_{B_x B_i}$, resulting in

$$\overline{i_{nR}^*} = \frac{4k_B T}{R_{Bv}} \Delta f \frac{e^{V_{B_x B_i}/V_T} - 1}{\frac{V_{B_x B_i}}{V_T}} \quad (42)$$

or the ac resistance $dV_{B_x B_i} / dI_{B_x B_i}$, resulting in

$$\overline{i_{nR}^*} = \frac{4k_B T}{R_{Bv}} \Delta f e^{V_{B_x B_i}/V_T}. \quad (43)$$

In Fig. 7, we compare the three results. The results coincide only for zero bias, where no dc current crowding is present. As one can see, to model the noise correctly it is not possible to just

use the standard noise expression for a resistor, as is being used in most models like Spice-Gummel-Poon. As can be expected, as a result of current crowding not only the resistance becomes nonlinear, also the expression for the noise really needs to be calculated separately.

VIII. RECTANGULAR GEOMETRY

For the rectangular geometry, many results are already known, starting with the work of Hauser [25]. For completeness' sake, we repeat the important ones. We then consider the large-current limit to be able to give an interpolation for $\overline{i_{nR}^*}$.

A. DC Current Crowding

The geometry we choose is a part of a rectangular emitter, having a length L_{em} and a width H_{em} . It is contacted only on one side, at $x = 0$. The line H_{em} is a symmetry axis of the transistor, of which we consider only half. It is known that $R_{Bv} = \rho H_{em} / 3L_{em}$. For this geometry, we have

$$J_{BE}(x) = \frac{2V_T}{\rho H_{em}^2} \left(\frac{Z}{\cos \left[Z \left(1 - \frac{x}{H_{em}} \right) \right]} \right)^2. \quad (44)$$

All expressions will be given in terms of an integration constant Z . We can find I_B and $V_{B_x B_i}$ from (7) and (22)

$$I_{B_x B_i} = \frac{2V_T}{3R_{Bv}} Z \tan Z, \quad e^{V_{B_x B_i}/V_T} = \frac{Z}{\sin Z \cos Z}. \quad (45)$$

We see that the relation between $I_{B_x B_i}$ and $V_{B_x B_i}$ can only be given implicitly in terms of Z . To circumvent the implicit analysis, an approximation is needed. We use that of Groendijk [28], discussed in Section VIII-D.

B. AC Current Crowding

For the differential (12), no solution is known that includes both high currents and nonzero frequency. The zero-frequency limit g_R of y_B can be found directly from the dc solution above. The solution for v at zero frequency is given by

$$v(x) = v_{B_x E} \frac{1 + \left(1 - \frac{x}{H_{em}} \right) \tan \left[Z \left(1 - \frac{x}{H_{em}} \right) \right]}{1 + \tan[Z]}. \quad (46)$$

We need this for the noise analysis.

The small-current limit leads to a normal transmission-line model and solutions have been known a long time [34]. For completeness sake, we just recall that in (26) we have $a = 1/5$ at low currents.

C. Noise Behavior

Just as in the case of a circular emitter, the only thing we need to calculate here is $\overline{i_{nR}^*}$. It follows from (34), with $g_s(r) = 1 - v(x)/v_{B_x E}$, where $v(x)$ is given in (46). It is possible to do the integration analytically, but the result is in terms of polylogarithmic functions that are too complicated to use in compact models. We will therefore present interpolation formulas in the next section.

D. Interpolation Formulas

Since it is not possible to give analytical results in the case of a rectangular emitter, we need to revert to interpolations. For these interpolations, we use the approach that Groendijk [28] used for dc current crowding. Groendijk calculated both the low-current limit and at the high-current limit and from those found an interpolation. We will extend this to ac and noise behavior. We will first analyze the high-current limit, where $Z \rightarrow \pi/2$ (the low current limit is simply $V_{B_x B_i} = I_{B_x B_i} R_{B_V}$ with corresponding ac and noise expressions).

For very high currents, the current will only be appreciable close the boundary. The various quantities will decrease over a length scale $1/k$. The value of k can be found from the decrease in current density close to the boundary

$$-\left. \frac{d \log J}{dx} \right|_{x=0} = \frac{Z \tan Z}{H_{em} \sin^2 Z}. \quad (47)$$

The value of k is then found by taking the limit of (47) for $Z \rightarrow \pi/2$. We find

$$k = \frac{3I_B R_{B_V}}{2H_{em} V_T}. \quad (48)$$

To find the base-to-emitter current density J_{BE} at high currents, we make use of the limit

$$\lim_{Z \rightarrow \pi/2} J_{BE}(x) \frac{V_T}{\rho} \frac{(1+kx)^2}{2k^2} = \left[\frac{\frac{\pi x}{2H_{em}}}{\sin\left(\frac{\pi x}{2H_{em}}\right)} \right]^2 \quad (49)$$

for J_{BE} given in (44). At high currents, only positions close to the boundary are relevant, so we only need to consider small values of x . The above limit is then equal to 1. Therefore, at high currents, we can write

$$J_{BE}(x) \simeq \frac{\rho}{V_T} \frac{2k^2}{(1+kx)^2}. \quad (50)$$

Again, we can find $e^{V_{B_x B_i}/V_T}$ from $J_{BE}(0)A_{em}/I_B$ —see (22). This leads to the relation

$$I_{B_x B_i} = \frac{2V_T}{3R_{B_V}} e^{V_{B_x B_i}/V_T}. \quad (51)$$

Using this high-current result, the interpolation Groendijk [28] found for all current levels is

$$I_{B_x B_i} = \frac{2V_T(e^{V_{B_x B_i}/V_T} - 1) + V_{B_x B_i}}{3R_{B_V}}. \quad (52)$$

This interpolation is correct within 4% for $V_{B_x B_i} > 0$ and within 10% for $V_{B_x B_i} < 0$. The expression has the correct limits for $|V| \ll V_T$ and for $|V| \gg V_T$ (hence including reverse operation). In Fig. 8, we show the differential resistance of both the exact solution and the interpolation formula. The correspondence is quite good for forward currents. For reverse currents, relevant for collector voltages above the collector-emitter breakdown [17], [18] it is still acceptable.

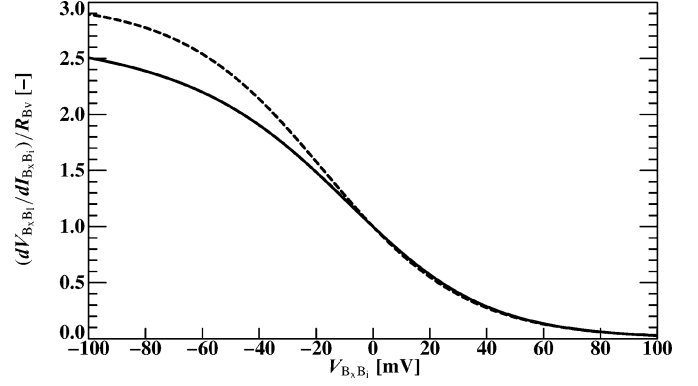


Fig. 8. Differential resistance $dV_{B_x B_i}/dI_{B_x B_i}$ normalized to R_{B_V} , both for the exact solution from (45) (solid) and from the interpolation (52). The x -axis is $V_{B_x B_i}$ for $V_T = 0.025$ V. For other values of V_T , the x -axis can be read as 0.025 V $\cdot (V_{B_x B_i}/V_T)$. Clearly, in forward mode the fit is much better, but even in reverse it is within 14%.

Next we extend this approach to ac behavior. As in the case of the circular emitter, we take $\gamma_B(\omega) = 1 + j\omega\tau$. The solution we find for the small-signal voltage in the high-current limit is

$$v(x) = \frac{v_{B_x E}}{1+kx} \left[1 - \frac{2}{3}j\omega\tau \ln(1+kx) \right] \quad (53)$$

again, to the first order in ω only. The small-signal admittance of the B_x - B_i branch is then

$$y_R = g_B \left(1 + \frac{1}{3}j\omega\tau \right). \quad (54)$$

This is exactly the same result as for the circular geometry at high currents ($g_B \gg 1/R_{B_V}$). The reason for this is that for extremely large current crowding the actual geometry is no longer relevant. Everything happens close to the boundary, and even the curvature of the boundary becomes irrelevant. This also means that (54) is valid at high currents for *all* geometries.

For the noise behavior at high currents, we use (19), (34), and (53) to find

$$\overline{i_{nR} i_{nR}^*} = \frac{10}{3} q I_B \Delta f = \frac{4k_B T}{R_{B_V}} \Delta f \cdot \frac{5e^{V_{B_x B_i}/V_T}}{9}. \quad (55)$$

Note that this result is the same as that of the circular geometry at high currents. Using the high-current limit, we propose as an interpolation formula for the noise the expression

$$\overline{i_{nR} i_{nR}^*} = \frac{4k_B T}{R_{B_V}} \Delta f \frac{5e^{V_{B_x B_i}/V_T} + 4}{9}. \quad (56)$$

This expression is not more than 6% from the exact result mentioned in Section VI-C (computed numerically and for positive base currents). We show the exact and interpolation formulas in Fig. 9.

IX. DISCUSSION OF ADDITIONAL PHYSICAL EFFECTS

In our analysis above, we assumed a rather ideal model for the intrinsic transistor. Here, we discuss the effect of things we

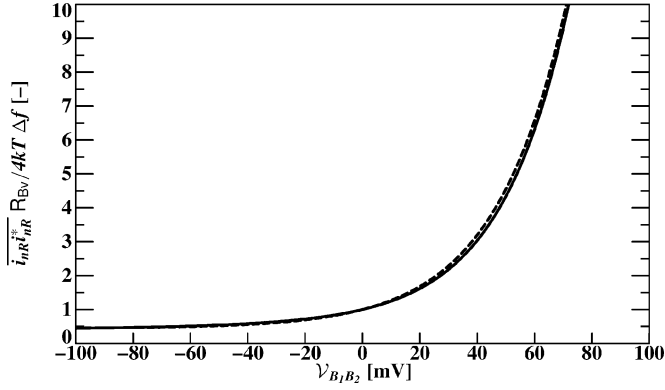


Fig. 9. Noise parallel to the base resistance $\overline{i_{nR}^*} R_{BV} / 4k_B T \Delta f$, both for the exact solution from (34) (solid) and from the interpolation (56) (dashed), as function of $V_{B_x B_i}$ (for $V_T = 25$ mV, see also Fig. 8). For values of $V_{B_x B_i} < -100$ mV both lines start to deviate from each other. The exact normalized noise goes rapidly to 4/9; the approximation goes slowly to 1/3.

neglected and some of the nonidealities on the current-crowding model.

We assumed that a lot of quantities are constant across the emitter. Examples are the current gain β (including Early effects), the base-emitter and base-collector depletion capacitances and the sheet resistance ρ . Although these quantities do depend on bias, we assume that the voltage drop over the base resistance is small enough—compared to the exponential behavior of the diode currents—to take them constant for our analysis. They are important, but do not have an effect on the way we model current crowding.

Let us consider the effect of avalanche current, which can be given as $(M - 1)I_C$. Here M is the multiplication factor. We assume weak avalanche, meaning that $M - 1 \ll 1$. The total base current is then

$$I_B = \frac{I_C}{\beta} - (M - 1)I_C = \frac{I_C}{\beta_{\text{eff}}}. \quad (57)$$

As we did for the current gain itself, we assume that the base-voltage dependence of the multiplication factor itself (over the emitter area) can be neglected. The base current is then still proportional to the collector current and still scales with e^{V/V_T} . All our derivations remain valid, and so do the expressions we found for the B_x - B_i branch in terms of $V_{B_x B_i}$. Modeling current crowding is therefore not influenced by weak avalanche, although the total base current becomes smaller or even negative. Note that the weak avalanche current also generates noise by itself [35]. This noise can be neglected compared to the shot noise of the collector (for weak avalanche), as long as the voltage is below breakdown [36], [37].

For a full compact model, it is necessary to consider also high-current effects. The relevant question for this work is whether high-current effects influence the expressions for current crowding. The base-emitter diode current itself does not show high-injection effects, due to the high emitter dope (and the fact that the base current is much smaller than the collector current). High-current effects do influence the modulation of the sheet resistance ρ . This can be taken into account, but

does not give very different results [32] from what we presented. We have seen that the intrinsic model can be considered independently of the current crowding model. In the case of high-injection effects, in the collector this is no longer fully true. The model becomes too complicated, however, if we try to add all the complexity of the collector current model to the current crowding model. We therefore do not take that into account.

Our general results are valid for all frequencies. In compact models, elements are described by currents or charges. This limits the description to the first order in frequency. (Higher order in frequency is a result of more internal nodes and hence more elements.) For practical implementation in compact models, our noise model therefore can be limited to the first order in frequency as well. We have shown results for the two relevant geometries in this limit.

We have not explicitly considered the base-collector depletion capacitance. This capacitance can be taken into account using appropriate expressions for the frequency dependence terms $\gamma_B(\omega)$ and $\gamma_C(\omega)$. (As before, we will take the base-collector capacitance to be constant as far as current crowding is concerned.) The fact that admittance y_B then also contains a term that is located between the base and collector instead of between the base and emitter does not change the derivations for current crowding. It only changes the implementation of the intrinsic model.

As a last point of discussion, we consider excess-phase shift. This is the effect that the collector current is delayed with respect to the emitter current. The effect this has on the noise was already taken into account by using a nonzero correlation between base and collector shot noise terms ($\gamma_{n,BC} \neq 0$). For implementation in the intrinsic model, two methods are possible. One of them is using $g_m e^{-j\omega\tau_d}$ in the small-signal circuit instead of g_m only. A large-signal version also exists [38] and is being used. An alternative is to use base-charge partitioning, in which case a part of the diffusion charge is put between base and collector (or emitter and collector) instead of between base and emitter. We have shown this term using the charge Q_{CE} in Fig. 3. In both cases, there is no effect on the current-crowding model, just as for the elements discussed above.

X. CONCLUSION

We have shown that it is possible to separate current-crowding effects from all the effects that play a role in the intrinsic transistor. This means that it is possible to make an accurate model of a transistor consisting of an intrinsic transistor containing all the terms that would be there without base resistance, and a branch that contains the base resistance and all its current-crowding effects. The intrinsic model is therefore independent of base resistance and current crowding. This gives a large freedom in making the intrinsic model as accurately as needed, without worrying about current crowding. The model for the dc current crowding and for the noise is independent of the intrinsic transistor. For ac current crowding, the most accurate model is found by using the base-emitter capacitance to model the charge in the B_x - B_i branch.

We have also shown that the noise in the B_x - B_i branch is more complicated than just the thermal noise of a lumped base resistance that is implemented in most compact models. We show how to calculate this noise as function of $V_{B_x B_i}$.

We have shown that for the most relevant geometries, that of a rectangular emitter and that of a small circular emitter, it is possible to give explicit expressions that model the current crowding. In both cases, the expressions found show a transition between linear low-current behavior and exponential high-current behavior. Also, negative base-currents are modeled. The approximate current-crowding expressions for dc, ac and noise behavior that are valid for the rectangular geometry have been implemented in the publicly available compact model Mextram [9].

APPENDIX A

DERIVATION OF TOTAL CURRENT NOISE SOURCES

Here, we present some of the details of the derivation in Section IV-C. The starting point are the differential equations (16). By eliminating the current \mathbf{j} , we find an equation for the voltage v_n , as follows:

$$[\nabla^2 - \gamma_B(\omega)F(\mathbf{r})] v_n(\mathbf{r}) = \nabla \cdot \mathbf{e}_{nR}(\mathbf{r}) + \rho j_{nB}(\mathbf{r}) \equiv s_n(\mathbf{r}). \quad (58)$$

We introduced the auxiliary function F , defined by

$$F(\mathbf{r}) = \frac{\rho}{V_T} J_{BE}(\mathbf{r}) \quad (59)$$

to make the notation below easier. The formal solution for v_n can be given in terms of a (complex) Green's function $G(\mathbf{r}|\mathbf{r}')$

$$v_n(\mathbf{r}) = \int G(\mathbf{r}|\mathbf{r}') s_n(\mathbf{r}') d\mathbf{r}'. \quad (60)$$

The differential equation for the Green's function is

$$[\nabla^2 - \gamma_B(\omega)F(\mathbf{r})] G(\mathbf{r}|\mathbf{r}') = \delta(\mathbf{r} - \mathbf{r}'). \quad (61)$$

We do not need an actual solution for this Greens function, but only use it in intermediate results. We do need the auxiliary function $y_s(\mathbf{r})$, defined by

$$y_s(\mathbf{r}) = - \int G(\mathbf{r}|\mathbf{r}') F(\mathbf{r}') d\mathbf{r}'. \quad (62)$$

This function y_s obeys the differential equation

$$[\nabla^2 - \gamma_B(\omega)F(\mathbf{r})] y_s(\mathbf{r}) = -F(\mathbf{r}). \quad (63)$$

Both for the Green's function and for y_s , the boundary condition is the same as for the voltage v_n of Section IV-C: they are zero on the boundary. Comparing (63) with (12), we see that we can express y_s in terms of the solution of v from Section IV-B

$$y_s(\mathbf{r}) = \frac{\left[1 - \frac{v(\mathbf{r})}{v_{B_x E}}\right]}{\gamma_B(\omega)}. \quad (64)$$

Using the Green's function for intermediate results, we can now express the total collector current noise and total base cur-

rent noise in terms of the auxiliary function y_s and of course in terms of the noise sources. We start with the base current and find

$$\begin{aligned} i_{TB} &= - \int \nabla \cdot \mathbf{j} d\mathbf{r} \\ &= \frac{\gamma_B(\omega)}{\rho} \int \int F(\mathbf{r}) G(\mathbf{r}|\mathbf{r}') s_n(\mathbf{r}') d\mathbf{r} d\mathbf{r}' + \int j_{nB}(\mathbf{r}) d\mathbf{r} \\ &= - \frac{\gamma_B(\omega)}{\rho} \int y_s(\mathbf{r}) [\nabla \cdot \mathbf{e}_{nR}(\mathbf{r}) + \rho j_{nB}(\mathbf{r})] d\mathbf{r} \\ &\quad + \int j_{nB}(\mathbf{r}) d\mathbf{r} \\ &= \frac{\gamma_B(\omega)}{\rho} \int \mathbf{e}_{nR}(\mathbf{r}) \cdot \nabla y_s(\mathbf{r}) d\mathbf{r} \\ &\quad + \int j_{nB}(\mathbf{r}) [1 - \gamma_B(\omega) y_s(\mathbf{r})] d\mathbf{r}. \end{aligned} \quad (65)$$

In the partial integrations above, we used the condition that y_s vanishes on the boundary. In the same way, we find for the total collector current

$$\begin{aligned} i_{TC} &= - \int \nabla \cdot \mathbf{j}_C d\mathbf{r} = \frac{\beta}{\rho} \gamma_C(\omega) \int \mathbf{e}_{nR}(\mathbf{r}) \cdot \nabla y_s(\mathbf{r}) d\mathbf{r} \\ &\quad - \beta \gamma_C(\omega) \int j_{nB}(\mathbf{r}) y_s(\mathbf{r}) d\mathbf{r} + \int j_{nC}(\mathbf{r}) d\mathbf{r}. \end{aligned} \quad (66)$$

APPENDIX B

CALCULATION OF SMALL-CURRENT RESISTANCE

We want to find the value of R_{Bv} , the effective resistance at small currents, in terms of the sheet resistance ρ . For small currents, the voltage in the base is almost constant (hence there is no dc current crowding). The local base-emitter voltage only differs by a small amount from $V_{B_x E}$ (which is yet unknown). For the function J_{BE} , defined in (5), we can therefore write

$$J_{BE}(V) \simeq \frac{I_B}{A_{em}} \left[1 + \frac{(V - V_{B_x E})}{V_T} \right]. \quad (67)$$

Next we express V in terms of the dimensionless quantity η as $V(\mathbf{r}) = V_{B_x E} - \eta(\mathbf{r}) I_B \rho$. Combining (7) and (67) leads to

$$V_{B_x E} - V_{B_i E} - \frac{I_B \rho}{A_{em}} \int_{A_{em}} \eta(\mathbf{r}) d\mathbf{r} = 0. \quad (68)$$

The effective resistance can then simply be given as

$$R_{Bv} = \frac{(V_{B_x E} - V_{B_i E})}{I_B} = \rho \int \eta(\mathbf{r}) \frac{d\mathbf{r}}{A_{em}}. \quad (69)$$

For finding $\eta(\mathbf{r})$, we need to solve (9), re-expressed in terms of η . We are still considering small currents so we only need the lowest relevant order of J_{BE} , which is here only the constant part of (67). The differential equation (9) then becomes

$$\nabla^2 \eta = -A_{em}^{-1}. \quad (70)$$

The boundary condition is that $\eta = 0$ at all points of the boundary, which follows from the boundary condition for V , i.e., $V = V_{B_x E}$.

As an example, we consider a rectangular emitter with the base connected at all sides (and not only at one or two sides as in Section VIII), for which the general expression is not well known. A general expression for the voltage in a rectangular geometry, such that the boundary condition is obeyed, is given by $V(\mathbf{r}) = V_{B_xE} - \eta(\mathbf{r})I_{B\rho}$, where

$$\eta(\mathbf{r}) = \sum_{m,n} a_{nm} \sin \frac{n\pi x}{H_{em}} \sin \frac{m\pi y}{L_{em}} \quad (71)$$

where L_{em} (H_{em}) is the emitter length (width). Solving the differential equation gives

$$a_{nm} = \left(\frac{2}{\pi}\right)^4 \frac{1}{nmH_{em}L_{em} \left(\frac{n^2}{H_{em}^2} + \frac{m^2}{L_{em}^2}\right)} \quad (72)$$

when both n and m are odd, and $a_{nm} = 0$ otherwise. One then finds

$$\begin{aligned} R_{Bv} &= \frac{\rho H_{em}}{L_{em}} \left(\frac{2}{\pi}\right)^6 \sum_{n,m \text{ odd}} \frac{1}{n^2 m^2 (n^2 + m^2 \alpha^2)} \\ &= \frac{\rho H_{em}}{L_{em}} \sum_{m \text{ odd}} \frac{16}{\alpha^3 m^5 \pi^5} \left(\frac{\alpha m \pi}{2} - \tanh \frac{\alpha m \pi}{2}\right) \end{aligned} \quad (73)$$

where $\alpha = H_{em}/L_{em}$. Equation (73) gives the analytical equation for the simulated results of [33].

For a square emitter contacted at all four sides, we find

$$R_{Bv} = \rho \sum_{m \text{ odd}} \frac{16}{m^5 \pi^5} \left(\frac{m\pi}{2} - \tanh \frac{m\pi}{2}\right) \simeq \frac{\rho}{28.45}. \quad (74)$$

From numerical device simulations, a value of $\rho/28.6$ was found in [31]. In the limit for $H_{em} \ll L_{em}$ ($\alpha \rightarrow 0$), we retrieve the well-known result for a long base contacted on two sides: $R_{Bv} = \rho H_{em}/12L_{em}$.

APPENDIX C

STATISTICAL PROPERTIES OF i_{nR}

In this Appendix, we calculate the statistical properties of i_{nR} . From the total noise currents, one can find the noise currents of the lumped circuit: i_{nC} from (27), i_{nB} from (30), and i_{nR} from (31). The correlation between i_{nR} and i_{nB} is then given by

$$\begin{aligned} \overline{i_{nR} i_{nB}^*} &= \int \int \overline{j_{nB}(\mathbf{r}) j_{nB}^*(\mathbf{r}')} \left[1 - \frac{y_R + y_B}{g_B} y_s(\mathbf{r})\right] d\mathbf{r} \\ &= \gamma_{n,BB}(\omega) 2q \Delta f \int J_{BE}(\mathbf{r}) \left[1 - \frac{y_R + y_B}{g_B} y_s(\mathbf{r})\right] d\mathbf{r} \\ &= \gamma_{n,BB}(\omega) 2q \Delta f \int J_{BE}(\mathbf{r}) \frac{y_B v(\mathbf{r}) - i_B}{y_B v_{B_xE} - i_B} d\mathbf{r} \\ &= 0. \end{aligned} \quad (75)$$

In the third step, we used (24) to express y_R in terms of $i_B = y_{TB} v_{B_xE}$ and (64) for the definition of y_s . In the last step, we used (7) and (13) for expression involving integrals over J_{BE} . In the same way, we find $\overline{i_{nR} i_{nC}^*} = 0$.

To calculate $\overline{i_{nR} i_{nR}^*}$, we need an intermediate result, using (18), (63), and (59) in the different steps, as follows:

$$\begin{aligned} &\frac{1}{\rho^2} \int \int \nabla y_s(\mathbf{r}) \cdot \overline{\mathbf{e}_{nR}(\mathbf{r}) \mathbf{e}_{nR}^*(\mathbf{r}')} \cdot \nabla y_s(\mathbf{r}) d\mathbf{r} d\mathbf{r}' \\ &= \frac{4k_B T}{\rho} \Delta f \int \nabla y_s \cdot \nabla y_s^* d\mathbf{r} = -\frac{4k_B T}{\rho} \Delta f \int y_s^*(\mathbf{r}) \nabla^2 y_s d\mathbf{r} \\ &= \frac{4k_B T}{\rho} \Delta f \int F(\mathbf{r}) y_s^*(\mathbf{r}) [1 - \gamma_B(\omega) y_s(\mathbf{r})] d\mathbf{r} \\ &= 2q \Delta f \int J_{BE}(\mathbf{r}) [y_s(\mathbf{r}) + y_s^*(\mathbf{r}) - [\gamma_B(\omega) + \gamma_B^*(\omega)] |y_s(\mathbf{r})|^2] d\mathbf{r}. \end{aligned} \quad (76)$$

In the second step, we used Green's first identity and in the third step the differential equation (64). In the last step, we used the fact that the result must be real. Using (76) we can find we find an expression for $\overline{i_{nR} i_{nR}^*}$. We can then use the same equations we used in deriving (75) to find

$$\begin{aligned} \overline{i_{nR} i_{nR}^*} &= 2k_B T \Delta f \left[(y_R + y_R^* + y_B + y_B^* - \gamma_{n,BB} g_B) \right. \\ &\quad \left. + (\gamma_{n,BB} - \gamma_B - \gamma_B^*) \frac{|y_R + y_B|^2}{V_T g_B^2} \int J_{BE}(\mathbf{r}) |y_s(\mathbf{r})|^2 d\mathbf{r} \right]. \end{aligned} \quad (77)$$

ACKNOWLEDGMENT

The author would like to thank A. Scholten for many valuable discussions about the calculation of noise in semiconductor devices.

REFERENCES

- [1] E. G. Nielsen, "Behavior of noise figure in junction transistors," *Proc. IRE*, vol. 45, pp. 957–963, 1957.
- [2] R. J. Hawkins, "Limitations of Nielsen's and related noise equations applied to microwave bipolar transistors and a new expression for the frequency and current dependent noise figure," *Solid-State Electron.*, vol. 20, pp. 191–196, 1977.
- [3] L. Escotte, J.-P. Roux, R. Plana, J. Graffeuil, and A. Gruhle, "Noise modeling of microwave heterojunction bipolar transistors," *IEEE Trans. Electron Devices*, vol. 42, pp. 883–889, May 1995.
- [4] K. Aufinger and M. Reisch, "RF noise models for bipolar transistors—A critical comparison," in *Proc. Bipolar Circuits and Technology Meeting*, 2001, pp. 110–113.
- [5] S. P. Voinigescu, M. C. Maliepaard, J. L. Showell, G. E. Babcock, D. Marchesan, M. Schröter, P. Schvan, and D. L. Harame, "A scalable high frequency noise model for bipolar transistors with application to optimal transistor sizing for low-noise amplifier design," *IEEE J. Solid-State Circuits*, vol. 32, pp. 1430–1439, Sept. 1997.
- [6] G. Niu, W. E. Ansley, S. Zhang, J. D. Cressler, C. S. Webster, and R. A. Groves, "Noise parameter optimization of UHV/CVD SiGe HBT's for RF and microwave applications," *IEEE Trans. Electron Devices*, vol. 46, pp. 1589–1598, Aug. 1999.
- [7] H. C. de Graaff and F. M. Klaassen, *Compact Transistor Modeling for Circuit Design*. Wien, Germany: Springer-Verlag, 1990.
- [8] J. Berkner, *Kompaktmodelle für Bipolartransistoren. Praxis der Modellierung, Messung und Parameterbestimmung—SGP, VBIC, HICUM und MEXTRAM (Compact Models for Bipolar Transistors. Practice of Modeling, Measurement and Parameter Extraction—SGP, VBIC, HICUM and MEXTRAM)* (in German). Renningen, Germany: Expert Verlag, 2002.
- [9] Information About the Most Recent Model Descriptions, Source Code, and Documentation. [Online]. Available: http://www.semiconductors.philips.com/Philips_Models

- [10] Model Definition and Other Information About Hicup. [Online]. Available: http://www.tee.et.tu-dresden.de/tee/eb/comp_mod.html
- [11] Y. Ciu, G. Niu, and D. L. Harnam, "An examination of bipolar transistor noise modeling and noise physics using microscopic noise simulations," in *Proc. Bipolar Circuits and Technology Meeting*, 2003, pp. 225–228.
- [12] J. A. Pals, "On the noise of a transistor with d.c. current crowding," *Philips Res. Repts.*, vol. 26, pp. 91–102, 1971.
- [13] G. Blasquez and J. Caminade, "Analyse des effets de la défocalisation du courant émetteur sur les mécanismes de conduction et de bruit de fond des transistors à jonctions (Analysis of defocusing effects of the emitter current on conduction mechanisms and noise phenomena in bipolar transistors)" (in French), *Phys. Stat. Sol. (a)*, vol. 31, pp. 713–728, 1975.
- [14] G. Blasquez, J. Caminade, and G. le Gac, "Analysis of the effects of current crowding on noise of transistors with a circular geometry. Application to transistor with any given geometry," *Physica B*, vol. 92, pp. 313–329, 1977.
- [15] G. Blasquez, J. Caminade, and K. M. van Vliet, "An accurate analysis of noise in rectangular bipolar transistors including current crowding," *Solid-State Electron.*, vol. 23, pp. 423–431, 1980.
- [16] G. Blasquez, J. Caminade, and G. le Gac, "Experimental study of the effects of current crowding on noise of bipolar transistors at intermediate frequencies," *Physica B*, vol. 94, pp. 359–365, 1978.
- [17] H.-M. Rein, T. Schad, and R. Zühlke, "Der einfluss des basisbahnwiderstandes und der ladungsträgermultiplikation auf das ausgangskennlinienfeld von planartransistoren (The influence of base resistance and carrier multiplication on the current-voltage characteristics of planar transistors)" (in German), *Solid-State Electron.*, vol. 15, pp. 481–500, 1972.
- [18] M. Rickelt, H.-M. Rein, and E. Rose, "Influence of impact-ionization-induced instabilities on the maximum usable output voltage of Si-bipolar transistors," *IEEE Trans. Electron Devices*, vol. 48, pp. 774–783, Apr. 2001.
- [19] A. van der Ziel, "Theory of shot noise in junction diodes and junction transistors," *Proc. IRE*, vol. 43, pp. 1639–1646, 1955.
- [20] A. van der Ziel and G. Bosman, "Accurate expression for the noise temperature of common emitter microwave transistors," *IEEE Trans. Electron Devices*, vol. ED-31, pp. 1280–1283, 1984.
- [21] G. Niu, J. D. Cressler, S. Zhang, W. E. Ansley, C. S. Webster, and D. L. Harnam, "A unified approach to RF and microwave noise parameter modeling in bipolar transistors," *IEEE Trans. Electron Devices*, vol. 48, pp. 2568–2574, Nov. 2001.
- [22] J. C. J. Paasschens, R. J. Havens, and L. F. Tiemeijer, "Modeling the correlation in the high-frequency noise of (heterojunction) bipolar transistors using charge-partitioning," in *Proc. Bipolar Circuits and Technology Meeting*, 2003, pp. 221–224.
- [23] A. van der Ziel, *Noise. Sources, Characterization, Measurement*. Englewood Cliffs, NJ: Prentice-Hall, 1970.
- [24] F. Bonani and G. Ghione, *Noise in Semiconductor Devices*. Berlin, Germany: Springer, 2001.
- [25] J. R. Hauser, "The effects of distributed base potential on emitter-current injection density and effective base resistance for stripe transistor geometries," *IEEE Trans. Electron Devices*, vol. ED-11, pp. 238–242, May 1964.
- [26] H. N. Ghosh, "A distributed model of the junction transistor and its application in the prediction of the emitter-base diode characteristic, base impedance, and pulse response of the device," *IEEE Trans. Electron Devices*, vol. ED-12, pp. 513–531, 1965.
- [27] E. S. Kohn, "Current crowding in a circular geometry," *J. Appl. Phys.*, vol. 42, pp. 2493–2497, 1971.
- [28] H. Groendijk, "Modeling base crowding in a bipolar transistor," *IEEE Trans. Electron Devices*, vol. ED-20, pp. 329–330, 1973.
- [29] J. E. Lary and R. L. Anderson, "Effective base resistance of bipolar transistors," *IEEE Trans. Electron Devices*, vol. ED-32, pp. 2503–2505, 1985.
- [30] A. Naimi, J. Boucher, and D. Andreu, "New spice model of total base resistance in bipolar transistors," *Solid-State Electron.*, vol. 36, pp. 639–641, 1993.
- [31] H.-M. Rein and M. Schröter, "Base spreading resistance of square-emitter transistors and its dependence on current crowding," *IEEE Trans. Electron Devices*, vol. 36, pp. 770–773, Apr. 1989.
- [32] M. Linder, F. Ingvarson, K. O. Jeppson, J. V. Grahn, S.-L. Zhang, and M. Östling, "On DC modeling of the base resistance in bipolar transistors," *Solid-State Electron.*, vol. 44, pp. 1411–1418, 2000.
- [33] M. Schröter, "Simulation and modeling of the low-frequency base resistance of bipolar transistors and its dependence on current and geometry," *IEEE Trans. Electron Devices*, vol. 38, pp. 538–544, 1991.
- [34] R. L. Pritchard, "Two-dimensional current flow in junction transistors at high frequencies," *Proc. IRE*, vol. 26, pp. 1152–1160, 1958.
- [35] R. J. McIntyre, "Multiplication noise in uniform avalanche diodes," *IEEE Trans. Electron Devices*, vol. ED-13, pp. 164–168, 1966.
- [36] D. Greenberg, S. Sweeney, G. Freeman, and D. Ahlgren, "Low-noise performance near BV_{CEO} in a 200 GHz SiGe technology at different collector design points," *IEEE MTT-S*, pp. 113–116, 2003.
- [37] J. C. J. Paasschens and R. de Kort, "Modeling the excess noise due to avalanche multiplication in (heterojunction) bipolar transistors," in *Proc. Bipolar Circuits and Technology Meeting*, 2004, to be published.
- [38] P. B. Weil and L. P. McNamee, "Simulation of excess phase in bipolar transistors," *IEEE Trans. Circuits Syst.*, vol. CAS-25, pp. 114–116, 1978.



Jeroen C. J. Paasschens was born in Valkenswaard, The Netherlands, in 1970. He received the M.Sc. degree in physics from the University of Nijmegen, Nijmegen, The Netherlands, in 1994, and the Ph.D. degree from the University of Leiden, Leiden, The Netherlands, in 1997.

He joined Philips Research Laboratories, Eindhoven, in 1998, and has been working on bipolar device modeling for circuit simulation. He is currently a member of the modeling and simulation program committee of the Bipolar/BiCMOS Circuits and Technology Meeting (BCTM).